Distributed Frequency Control of Inertia-Less AC Microgrids

Stanton T. Cady, Christoforos N. Hadjicostis, and Alejandro D. Domínguez-García

Abstract— **In this paper, we introduce a generation control architecture for microgrids that ensures stable and synchronized operation at a specific frequency. We also propose a distributed implementation of this architecture that relies on two distributed algorithms that adhere to a communication network interconnecting the controllers present at each bus. The first algorithm enables the generators to determine set-points that result in stable and synchronized operation given a known set of load bus power demands, whereas the second one enables the generators to drive their commands to the aforementioned set-points. We demonstrate our proposed controller and its distributed implementation via numerical simulations.**

I. Introduction

While generation control of large power systems is a well-studied problem (see, e.g., [1]), the unique characteristics of microgrids, together with the desire to increase reliability and adaptability, serve to motivate the development of new generation control paradigms and topologies. In particular, whereas existing architectures utilized for large power system generation control typically rely on a centrally located computer, several distributed alternatives have been proposed for microgrids (see, e.g., [2], [3]). By combining information received from neighboring controllers with local computations, such architectures can replicate the functionality of their centralized counterparts without requiring complete information about the number, type, or capabilities of the generation units. Additionally, elimination of the central processor and the communication network that connects it to each generator increases adaptability to failures.

Irrespective of system size or the type of control architecture used, all ac power systems have similar control objectives. More specifically, (i) generation and demand must be balanced, (ii) frequency must be regulated, and (iii) costs associated with generation should be minimized. In the case of microgrids, primary generation control—as the system designed to achieve the first objective is typically called—can generally be handled in a manner similar to that in large power systems (see, e.g., [2]). Moreover, although objective (iii) remains important in microgrids, assigning costs to energy sources such as photovoltaic arrays is not as straightforward as is the case for large-scale generation. While it is possible to specify suitable cost functions for generation units with ill-defined energy costs (see, e.g., [4]), controlling a microgrid in such a way that the frequency is regulated, i.e., meets objective (ii), and results in stable and synchronized operation should be the primary objective [5].

Although control for microgrids and distributed control for large power networks has been thoroughly discussed in the literature (see, e.g., [6], [7] and the references therein), the task of designing a control scheme for frequency regulation that achieves the aforementioned properties has received limited attention thus far. In our previous work in [4], we proposed a distributed control architecture that is suitable for regulating the frequency in a microgrid. While we experimentally showed that the architecture presented therein was sufficient to drive the frequency error to zero, the approach we took did not necessarily result in stable and synchronized operation. The authors in [8] similarly propose a distributed control architecture for regulating the weighted average of the system frequency, which they analytically show to be exponentially stable, but which may not necessarily result in synchronized operation. The work in [9] provides the conditions under which a system of interconnected oscillators, such as the loads and generators in an inertia-less microgrid, is stable and synchronized, but, to our knowledge, no previous work has proposed a controller that ensures these conditions are satisfied; the objective of the work we present in this paper is to develop such a controller.

Specifically, in this paper, we propose a feedback control scheme suitable for inertia-less microgrids that drives the system to a stable operating point wherein the loads and generators are synchronized to a common, pre-specified frequency. The objectives of our proposed controller are achieved by tracking generation set-points that have been determined *a priori* while rejecting disturbances, e.g., load changes, so as to maintain a desired frequency; the predetermined set-points are chosen such that, for bounded disturbances, stable and synchronized operation results. Additionally, we propose a distributed implementation of the control architecture that relies on a communication network interconnecting local controllers present at each bus rather than a centrally located computer. Our distributed implementation is comprised of two algorithms: (i) an iterative algorithm that enables the local controllers to determine set-points that result in stable and synchronized operation given a known set of load bus power demands, and (ii) an algorithm that uses ratio consensus (see, e.g., [10]) as a primitive to reject disturbances by driving the average weighted frequency error to zero.

S. T. Cady and A. D. Domínguez-García are with the Department of Electrical and Computer Engineering at the University of Illinois at Urbana-Champaign, Urbana, IL 61801, USA. E-mail: {scady2,aledan}@ILLINOIS.EDU.

C. N. Hadjicostis is with the Department of Electrical and Computer Engineering at the University of Cyprus, Nicosia, Cyprus, and also with the Department of Electrical and Computer Engineering at the University of Illinois at Urbana-Champaign, Urbana, IL 61801, USA. E-mail: chadjic@UCY.AC.CY.

II. Preliminaries

We begin this section by introducing a model to represent the dynamics of a microgrid with inertia-less power generation sources. Next, we describe a graph-theoretic model to represent the interconnections between buses in the power network. Finally, we outline the conditions under which the microgrid is synchronized and stable. We use the graph-theoretic model and the conditions for synchronized and stable operation provided in this section when developing our proposed control scheme in Section III.

A. Microgrid Dynamical Model

Consider an inertia-less microgrid with $n = m + l$ buses. Without loss of generality, assume that m of these buses, indexed by $\mathcal{V}_g = \{1, 2, \ldots, m\}$, have only generators attached to them, and that the remaining l buses, indexed by $\mathcal{V}_l = \{m+1, m+2, \ldots, m+l\}$, have only loads attached to them. Further assume that the generators have no internal impedance, i.e., $z_i = 0$, $i \in \mathcal{V}_g$; the power network is linear and lossless, i.e., $r_{ij} = 0$, $i, j = 1, 2, \ldots, n$; and the voltage magnitude at all buses is constant and unity, i.e., $V_i = 1$ pu, $i = 1, 2, \ldots, n$.[1]

At time $t \geq 0$, let $\theta_i(t)$ denote the voltage angle at bus i, and $u_i(t)$ denote the set-point of a generator at bus $i \in \mathcal{V}_g$, with $0 \leq \underline{u}_i \leq u_i(t) \leq \overline{u}_i$, where $\underline{u}_i$ and $\overline{u}_i$ are the minimum and maximum output of generator i, respectively. Additionally, let $\ell_i \geq 0$ denote the real power demand of a load at bus $i \in \mathcal{V}_l$, and assume it to be constant; then, the dynamics of the microgrid can be described by [8]:

$$D_i \frac{d\theta_i(t)}{dt} = u_i(t) - \sum_{j=1}^{n} B_{ij} \sin(\theta_i(t) - \theta_j(t)), \qquad (1)$$

for $i \in \mathcal{V}_g$, and

$$D_i \frac{d\theta_i(t)}{dt} = -\ell_i - \sum_{j=1}^{n} B_{ij} \sin(\theta_i(t) - \theta_j(t)), \qquad (2)$$

for $i \in \mathcal{V}_l$, where $D_i > 0$, and B_{ij} is the (i, j) entry of the susceptance matrix, B, i.e., the imaginary part of the network admittance matrix (see, e.g., [11]).

If we let $\theta(t) = \left[\theta_1(t), \theta_2(t), \ldots, \theta_n(t)\right]^{\mathrm{T}}$, $u(t) = \left[u_1, u_2, \ldots, u_m\right]^{\mathrm{T}}$, and $\ell = \left[\ell_{m+1}, \ell_{m+2}, \ell_n\right]^{\mathrm{T}}$, then, we can rewrite (1) – (2) in matrix form as

$$D \frac{d\theta(t)}{dt} = \begin{bmatrix} u(t) \\ -\ell \end{bmatrix} - H(\theta(t)), \qquad (3)$$

where $D = \mathrm{diag}(D_1, D_2, \ldots, D_n)$, and $H(\theta(t)) = \left[H_1(\theta(t)), H_2(\theta(t)), \ldots, H_n(\theta(t))\right]^{\mathrm{T}}$, with $H_i(\theta(t)) = \sum_{j=1}^{n} B_{ij} \sin(\theta_i(t) - \theta_j(t))$.

[1] While these assumptions may not hold under extreme conditions, we consider operation around a nominal operating point where they are justifiable approximations of the actual network behavior (see, e.g., [9]).

B. Graph-Theoretic Network Model

Given (1) – (2) (or more compactly as written in (3)), let $\mathcal{V} = \mathcal{V}_g \cup \mathcal{V}_l$, and $\mathcal{E} \subseteq \{\{i, j\} \mid i, j \in \mathcal{V}, i \neq j\}$, where $\{i, j\} \in \mathcal{E}$, $i \neq j$, if there is an interconnection between buses i and j, i.e., $B_{ji} = B_{ij} \neq 0$. Furthermore, let $A = B - \mathrm{diag}(\{B_{ii}\})$, where $\mathrm{diag}(\{B_{ii}\})$ is a diagonal matrix of self-susceptances; then, $G = (\mathcal{V}, \mathcal{E}, A)$ is an undirected, connected, and weighted simple graph representing the interconnections between buses in the microgrid. Based upon the definition of the adjacency matrix, $A \in \mathbb{R}^{n \times n}$, the edge weights of G correspond to the admittances of the interconnections between buses. For each node $i \in \mathcal{V}$, we denote the set of nodes for which $B_{ij} \neq 0$ as $\mathcal{N}_i := \{j \in \mathcal{V} : \{i, j\} \in \mathcal{E}\}$. If we assign an arbitrary direction to each edge $e = \{i, j\} \in \mathcal{E}$, the oriented incidence matrix of G, $M \in \mathbb{R}^{|\mathcal{V}| \times |\mathcal{E}|}$, is defined component-wise as follows:

$$M_{ie} = \begin{cases} -1, & \text{if } i \text{ is the sink node,} \\ 1, & \text{if } i \text{ is the source node,} \\ 0, & \text{if } e \text{ is not incident to node } i. \end{cases}$$

The Laplacian matrix of G is defined as $L = M\mathrm{diag}(\{B_{ij}\})M^{\mathrm{T}}$, where $\mathrm{diag}(\{B_{ij}\})$ is a diagonal matrix of non-zero susceptances on each edge $e = \{i, j\} \in \mathcal{E}$ (in the order in which edges e appear in M).

C. Conditions for Synchronization and Stability

The objective of the control architecture presented in Section III is to adjust the set-points of the generation units in a microgrid, i.e., the $u_i(t)$'s, such that the system reaches a stable operating point wherein the frequency of all the buses is synchronized and regulated to some reference, ω_0. Without loss of generality, if we transform the system to a reference frame rotating at ω_0, the frequency regulation objective is equivalent to choosing the generation set-points such that $\frac{d\theta_i}{dt} \to 0$, for all i. Thus, the control objectives can be summarized by the following properties (see, e.g., [9]):

- **P1.** The system in (1) – (2) reaches an operating point $\theta^* = \left[\theta_1^*, \theta_2^*, \ldots, \theta_n^*\right]^{\mathrm{T}}$ such that the angular velocities of all the buses are zero, i.e., $\frac{d\theta_i}{dt} \to 0$ as $t \to \infty$ for all i.
- **P2.** The system in (1) – (2) is stable around the operating point θ^*, i.e., $-\frac{dH(\theta(t))}{d\theta}\Big|_{\theta=\theta^*} \preceq 0$.
- **P3.** The operating point θ^* is phase cohesive, i.e., for some angle $\gamma \in [0, \pi/2)$, $|\theta_i^* - \theta_j^*| \leq \gamma$ for every $i, j \in \mathcal{V}$.

The task of finding control set-points that meet Properties P1 – P3 without violating generation limits is equivalent to finding a solution to the following feasibility problem:

$$\begin{aligned} \text{find} \quad & u \\ \text{subject to} \quad & \sum_{i=1}^{m} u_i = \sum_{i=m+1}^{n} \ell_i \\ & \left\| M^{\mathrm{T}} L^{\dagger} \begin{bmatrix} u \\ -l \end{bmatrix} \right\|_{\infty} < \sin(\gamma) \\ & \underline{u}_i \leq u_i \leq \overline{u}_i, \, \forall i \in \mathcal{V}_g, \end{aligned} \qquad (4)$$

for some $\gamma \in [0, \pi/2)$, where $L^{\dagger}$ denotes the *Moore-Penrose pseudo inverse* of L.

III. Control Scheme

In this section, we propose a feedback control scheme that serves to drive the frequency error in a microgrid to zero while ensuring stability and synchronism. Our approach relies on a discrete-time proportional integral (PI) controller that is executed over several rounds; the controller tracks generation set-points determined beforehand to be within limits and to separately meet the following two objectives:

O1. regulate frequency, i.e., satisfy Property P1; and

O2. ensure stability and synchronism, i.e., satisfy Properties P2 and P3.

More specifically, integral action is used to satisfy Objective O1 by driving the weighted average frequency error to zero while proportional control is used to satisfy Objective O2 by tracking predetermined set-points which are known to correspond to stable and synchronized operation within individual generation limits. Thus, the control architecture will maintain stability and synchronism for bounded disturbances while regulating the frequency to the desired value.

Let $\Delta\overline{\omega}(t)$ denote the average frequency error in the microgrid in (1) – (2), weighted by the D_i's of the generators and loads, i.e., $\Delta\overline{\omega}(t) := \frac{\sum_{i=1}^{n} D_i \frac{d\theta_i(t)}{dt}}{\sum_{i=1}^{n} D_i}$. Then, the goal of Objective O1 is to drive $\Delta\overline{\omega}(t) \to 0$ as $t \to \infty$. By summing all the equations in (1) with all the equations in (2), it is easy to see that

$$\Delta\overline{\omega}(t) = \frac{1}{\sum_{i=1}^{n} D_i} \left(\sum_{i=1}^{m} u_i(t) - \sum_{i=m+1}^{n} \ell_i \right), \tag{5}$$

which implies that if $\Delta\overline{\omega}(t) \to 0$ as $t \to \infty$, then

$$\lim_{t\to\infty} \sum_{i=1}^{m} u_i(t) = \sum_{i=m+1}^{n} \ell_i.$$

To achieve Objectives O1 and O2, the set-point of each generator in our proposed strategy is updated every T_0 units of time and held constant for the subsequent T_0 time units. Let $r = 0, 1, 2, \ldots$ index the rounds at which the set-points are updated, where $t_r = rT_0$ is the time at the beginning of round r, and define $u_i^r = u_i(t)$, $t_r \le t < t_{r+1}$ to be the set-point of generator i during round r. Furthermore, let $u^* = \left[u_1^*, u_2^*, \ldots, u_m^*\right]^{\mathrm{T}}$ be a vector of set-points that satisfies the feasibility problem in (4) (an algorithm for finding such set-points is provided in Section IV); then, each generator adjusts its set-point at each round to be

$$u_i^r = u_i^* + \kappa_i e_i^r, \tag{6}$$

where e_i^r is updated according to the following recursive relationship:

$$e_i^{r+1} = e_i^r + \alpha_i \Delta\overline{\omega}^r, \tag{7}$$

with $\Delta\overline{\omega}^r = \Delta\overline{\omega}(t)$, $t_r \le t < t_{r+1}$. The response of the closed-loop system can be altered by adjusting κ_i and α_i in (6) and (7), respectively; however, these gains must be chosen such that Properties P1 – P3 are achieved. Next, we provide some criteria for choosing appropriate gains.

By combining (5) and (6) for $t_{r+1} \le t < t_{r+2}$, we have that $\Delta\overline{\omega}(t) = \Delta\overline{\omega}^{r+1}$ and

$$\begin{aligned}
\Delta\overline{\omega}^{r+1} &= \overline{D} \left(\sum_{i=1}^{m} u_i^{r+1} - \sum_{i=m+1}^{n} \ell_i \right), \\
&= \overline{D} \left(\sum_{i=1}^{m} (u_i^* + \kappa_i e_i^{r+1}) - \sum_{i=m+1}^{n} \ell_i \right), \\
&= \overline{D} \left(\sum_{i=1}^{m} (\kappa_i e_i^r + \kappa_i \alpha_i \Delta\overline{\omega}^r) + \sum_{i=1}^{m} u_i^* - \sum_{i=m+1}^{n} \ell_i \right),
\end{aligned} \tag{8}$$

where $\overline{D} := \frac{1}{\sum_{i=1}^{n} D_i}$. Given the assumption that u^* satisfies (4), we have that $\sum_{i=1}^{m} u_i^* = \sum_{i=m+1}^{n} \ell_i$; thus,

$$\Delta\overline{\omega}^{r+1} = \overline{D} \sum_{i=1}^{m} (\kappa_i e_i^r + \kappa_i \alpha_i \Delta\overline{\omega}^r). \tag{9}$$

Let $\alpha = \left[\alpha_1, \alpha_2, \ldots, \alpha_m\right]^{\mathrm{T}}$ and $\kappa = \left[\kappa_1, \kappa_2, \ldots, \kappa_m\right]^{\mathrm{T}}$; then, by stacking (7) and (9), we obtain

$$\begin{bmatrix} e^{r+1} \\ \Delta\overline{\omega}^{r+1} \end{bmatrix} = \underbrace{\begin{bmatrix} I_{m\times m} & \alpha \\ \overline{D}\kappa^{\mathrm{T}} & \overline{D}\kappa^{\mathrm{T}}\alpha \end{bmatrix}}_{:=\Phi\in\mathbb{R}^{(m+1)\times(m+1)}} \begin{bmatrix} e^r \\ \Delta\overline{\omega}^r \end{bmatrix}, \tag{10}$$

where $I_{m\times m}$ is the $m \times m$-dimensional identity matrix. We can ensure that the system in (10) is stable by choosing α_i's and κ_i's such that the transition matrix, Φ, has eigenvalues with magnitudes strictly smaller than one. Given such a set of gains, it follows that $\lim_{r\to\infty} e_i^r = 0$, $i \in \mathcal{V}_g$, and $\lim_{r\to\infty} \Delta\overline{\omega}^r = 0$; furthermore, from (6) and (7), we have that $\lim_{r\to\infty} u_i^r = u_i^* + \kappa_i e_i^{r-1} + \kappa_i \alpha_i \Delta\overline{\omega}^{r-1} = u_i^*$, $i \in \mathcal{V}_g$.

IV. Distributed Implementation

Although the discussion in the previous section may imply that global information is required by each node to implement the control in (6) – (7), in this section, we introduce two algorithms that allow the nodes to distributively acquire the information necessary to implement such a control scheme. The first algorithm enables the nodes to acquire the value of the average frequency error, $\Delta\overline{\omega}^r$, at each round. The second algorithm enables the nodes to iteratively determine a set of network flows that allow the power demanded by the loads to be met without violating any generator or line limits; at the end of this iterative process, the generator nodes obtain set-points that satisfy (4).

A. Weighted Average Frequency Error

By inspecting (5), it is easy to see that the value of $\Delta\overline{\omega}(t)$ is defined as the ratio of sums of values known by each of the nodes. More specifically, for $t_r \le t < t_{r+1}$, if we let

$$x_i^r = \begin{cases} u_i^r, & \text{if } i \in \mathcal{V}_g, \\ -\ell_i, & \text{if } i \in \mathcal{V}_l, \end{cases}$$

we see that $\Delta\overline{\omega}^r = \frac{\sum_{i=1}^{n} x_i^r}{\sum_{i=1}^{n} D_i}$.

While it seems as though a centralized entity with knowledge of x_i^r and D_i for every $i \in \mathcal{V}$ is required to compute

$\Delta\overline{\omega}^r$, the so-called ratio-consensus algorithm (see, e.g., [10]) can be used to allow each node to asymptotically obtain the value of $\Delta\overline{\omega}^r$ at each round r. In ratio consensus, each node i maintains two states, $y_i^r[k]$ and $z_i^r[k]$, and iteratively updates them for $k = 0, 1, 2, \ldots$. If the states are initialized as $y_i^r[0] = x_i$ and $z_i^r[0] = D_i$ and updated according to

$$y_i^r[k+1] = \sum_{j \in \mathcal{N}_i \cup \{i\}} \frac{1}{|\mathcal{N}_j| + 1} y_j^r[k], \tag{11}$$

$$z_i^r[k+1] = \sum_{j \in \mathcal{N}_i \cup \{i\}} \frac{1}{|\mathcal{N}_j| + 1} z_j^r[k], \tag{12}$$

it follows from the analysis in [10] that

$$\lim_{k \to \infty} \frac{y_i^r[k]}{z_i^r[k]} = \frac{\sum_{l=1}^n y_l^r[0]}{\sum_{l=1}^n z_l^r[0]} = \Delta\overline{\omega}^r, \, \forall i \in \mathcal{V}. \tag{13}$$

Although the result in (13) implies that the process to obtain $\Delta\overline{\omega}^r$ must extend over an infinite number of iterations, in our work in [12], we presented a variant of the ratio-consensus algorithm that allows each node to compute $\Delta\overline{\omega}^r$ to within a pre-specified accuracy in finite-time. In the simulation results presented in Section V, we make use of this variant.

B. Feasible Flow Algorithm

For the algorithm introduced in this section, we assume that each node $i \in \mathcal{V}$ knows the value of D_i, the values of the susceptances, B_{ij}, of the lines interconnecting it to each $j \in \mathcal{N}_i$, and that each load $i \in \mathcal{V}_l$ knows the amount of power it draws, ℓ_i. Furthermore, we will make use of an auxiliary graph, denoted by G_f, that allows us to represent the power transfer limits of each line in the microgrid and the limits of the generation units in a unified manner. This auxiliary graph is only used to simplify the description of the algorithm; any computations associated with auxiliary nodes will be subsumed by the local controller of its corresponding generator or load. Additionally, for the purposes of the algorithm, it is assumed that the total power demanded by the loads can be met by the generation units, i.e., $\sum_{i=1}^m \underline{u}_i \leq \sum_{i=m+1}^n \ell_i \leq \sum_{i=1}^m \overline{u}_i$.

From the undirected graph $G = (\mathcal{V}, \mathcal{E})$ defined in Section II-B, consider the spanning supergraph $G' = (\mathcal{V}', \mathcal{E}')$, where an auxiliary node is added for each generator and load in the microgrid and an undirected edge is added connecting each auxiliary node to its corresponding generator or load node, i.e., $\mathcal{V}' = \{i' : i \in \mathcal{V}\} \cup \mathcal{V}$ and $\mathcal{E}' = \{\{i', i\} : i \in \mathcal{V}\} \cup \mathcal{E}$. Then, let $G_f = (\mathcal{V}_f, \mathcal{E}_f)$ be a directed graph where $\mathcal{V}_f = \mathcal{V}'$ and the edge set consists of the natural and reverse orientation of the edges in G', i.e., $\mathcal{E}_f = \{(i,j), (j,i) : \{i,j\} \in \mathcal{E}'\}$.

Given the graph G_f, let $F \in \mathbb{R}^{|\mathcal{V}_f| \times |\mathcal{V}_f|}$ be a matrix of power flows along directed edges $(i,j) \in \mathcal{E}_f$, where the element f_{ij} corresponds to a flow from node j to node i, i.e., the injection into i from j. Then, from the model of the power network given in (1) – (2), and for operating conditions approaching the limit of the phase angle difference in Property P3, i.e., for $\gamma \to \pi/2$, we see that the power flow along edge $(i,j) \in \mathcal{E}_f$, $i, j \in \mathcal{V} \setminus \mathcal{V}_f$, is limited by the susceptance of the line, B_{ij}. Furthermore, for the generators and their corresponding auxiliary nodes, we see that the flow injected to $i \in \mathcal{V}_g$ from $j \in \mathcal{V}_f \setminus \mathcal{V}$ along edge $(i,j) \in \mathcal{E}_f$ is bounded from below by $\underline{u}_i$ and above by $\overline{u}_i$. Similarly, for the loads and their corresponding auxiliary nodes, the flow injected to $i \in \mathcal{V}_f \setminus \mathcal{V}$ from $j \in \mathcal{V}_l$ along edge $(i,j) \in \mathcal{E}_f$ must be equal to ℓ_j.

Let $\underline{F}, \overline{F} \in \mathbb{R}^{|\mathcal{V}_f| \times |\mathcal{V}_f|}$ be matrices representing the minimum and maximum flows between nodes in G_f; from the discussion above, for a flow injected to i from j, $\underline{F}$ is defined element-wise as

$$\underline{f}_{ij} = \begin{cases} -B_{ij}, & \text{if } i,j \in \mathcal{V} \setminus \mathcal{V}_f, \\ \underline{u}_i, & \text{if } i \in \mathcal{V}_g \text{ and } j \in \mathcal{V}_f \setminus \mathcal{V}, \\ \ell_j, & \text{if } i \in \mathcal{V}_f \setminus \mathcal{V} \text{ and } j \in \mathcal{V}_l, \\ 0, & \text{otherwise,} \end{cases}$$

and the elements of $\overline{F}$ are

$$\overline{f}_{ij} = \begin{cases} B_{ij}, & \text{if } i,j \in \mathcal{V} \setminus \mathcal{V}_f, \\ \overline{u}_i, & \text{if } i \in \mathcal{V}_g \text{ and } j \in \mathcal{V}_f \setminus \mathcal{V}, \\ \ell_j, & \text{if } i \in \mathcal{V}_f \setminus \mathcal{V} \text{ and } j \in \mathcal{V}_l, \\ 0, & \text{otherwise.} \end{cases}$$

[Note that for each bound specified above, the reverse flow, i.e., the flow from i injected to j, is limited by the respective additive inverse, i.e., $\overline{f}_{ji} = -\underline{f}_{ij}$ and $\underline{f}_{ji} = -\overline{f}_{ij}$.] Then, the objective of obtaining generator set-points that satisfy (4) is equivalent to finding a matrix F such that

$$\begin{aligned} &\underline{F} \leq F \leq \overline{F}, \\ &F 1_{|\mathcal{V}_f|} = 0_{|\mathcal{V}_f|}, \\ &F = -F^{\mathrm{T}}, \end{aligned} \tag{14}$$

where $1_{|\mathcal{V}_f|}$ is the $|\mathcal{V}_f|$-dimensional all-ones vector.

To distributively compute a set of feasible flows that satisfy (14), each node maintains an estimate of each flow injected into it, i.e., $f_{ij}[k,s]$ for $j \in \mathcal{N}_i$, which it updates iteratively for $k = 0, 1, 2, \ldots$ and for $s = 1, 2, 3$ following the three-step process below, the pseudocode of which is given in Algorithm 1.

[**Step** $s = 1$] Each node i determines the sum of the in- and out-flows as computed during the last step of the previous iteration. If there is a mismatch between the summations, each flow is adjusted to ensure that the total in- and out-flows are balanced. Specifically, let $\mathcal{N}_i^-[k] := \{j : f_{ij}[k,3] > 0\}$ be the set of nodes injecting flows into node i and $\mathcal{N}_i^+[k] := \{j : f_{ij}[k,3] < 0\}$ be the set of nodes into which node i is injecting flows; the remaining flows are in the set $\mathcal{N}_i^0[k] = \mathcal{N}_i \setminus (\mathcal{N}_i^+[k] \cup \mathcal{N}_i^-[k])$. Note that for some k, $\mathcal{N}_i^-[k]$, $\mathcal{N}_i^+[k]$, or $\mathcal{N}_i^0[k]$ may possibly be empty. Furthermore, let $\Sigma_i^-[k] := \sum_{j \in \mathcal{N}_i^-[k]} f_{ij}[k,3]$ and $\Sigma_i^+[k] := \sum_{j \in \mathcal{N}_i^+[k]} f_{ij}[k,3]$ be the sum of the in- and out-flows, and define $e_i[k] := ||\Sigma_i^+[k]| - |\Sigma_i^-[k]||$ to be the magnitude of the mismatch between the in- and out-flows. Then, each node i updates the flow for each

Algorithm 1: Distributed feasible flow algorithm

Each node $i \in \mathcal{V}_f$ **separately does the following:**
Input: $\underline{f}_{ij}, \overline{f}_{ij}$, $j \in \mathcal{N}_i$
Output: f_{ij}, $j \in \mathcal{N}_i$

begin
  Set $f_{ij}[0] = 0$, for all i, j
  foreach *iteration,* $k = 0, 1, ..., k_o$ **do**
    Determine: $\mathcal{N}_i^+[k]$, $\Sigma_i^+[k]$, $\mathcal{N}_i^-[k]$, $\Sigma_i^-[k]$, $\mathcal{N}_i^0[k]$, and $e_i[k]$
    if $|\Sigma_i^+[k]| > |\Sigma_i^-[k]|$ **then**
      foreach $j \in \mathcal{N}_i^+[k]$ **do**
        $f_{ij}[k+1,1] = f_{ij}[k,3] + \frac{e_i[k]}{2|\mathcal{N}_i^+[k]|}$
      foreach $j \in \mathcal{N}_i^-[k] \cup \mathcal{N}_i^0[k]$ **do**
        $f_{ij}[k+1,1] = f_{ij}[k,3] + \frac{e_i[k]}{2(|\mathcal{N}_i^-[k]|+|\mathcal{N}_i^0[k]|)}$
    else if $|\Sigma_i^+[k]| < |\Sigma_i^-[k]|$ **then**
      foreach $j \in \mathcal{N}_i^+[k] \cup \mathcal{N}_i^0[k]$ **do**
        $f_{ij}[k+1,1] = f_{ij}[k,3] - \frac{e_i[k]}{2(|\mathcal{N}_i^+[k]|+|\mathcal{N}_i^0[k]|)}$
      foreach $j \in \mathcal{N}_i^-[k]$ **do**
        $f_{ij}[k+1,1] = f_{ij}[k,3] - \frac{e_i[k]}{2|\mathcal{N}_i^-[k]|}$
    foreach $j \in \mathcal{N}_i$ **do**
      $f_{ij}[k+1,2] = \frac{1}{2}(f_{ij}[k+1,1] - f_{ji}[k+1,1])$
    foreach $j \in \mathcal{N}_i$ **do**
      if $f_{ij}[k+1,2] > \overline{f}_{ij}$ **then**
        $f_{ij}[k+1,3] = \overline{f}_{ij}$
      else if $f_{ij}[k+1,2] < \underline{f}_{ij}$ **then**
        $f_{ij}[k+1,3] = \underline{f}_{ij}$
      else
        $f_{ij}[k+1,3] = f_{ij}[k+1,2]$

adjacent node $j \in \mathcal{N}_i$ as $f_{ij}[k+1,1] = f_{ij}[k,3] + \Delta f_{ij}[k]$, where

$$\Delta f_{ij}[k] = \begin{cases} -\frac{1}{2}\frac{e_i[k]}{|\mathcal{N}_i^+[k]|+|\mathcal{N}_i^0[k]|}, & \text{if } j \in \mathcal{N}_i^+[k] \cup \mathcal{N}_i^0[k] \\ -\frac{1}{2}\frac{e_i[k]}{|\mathcal{N}_i^-[k]|}, & \text{otherwise,} \end{cases}$$

if $|\Sigma_i^-[k]| > |\Sigma_i^+[k]|$, and

$$\Delta f_{ij}[k] = \begin{cases} \frac{1}{2}\frac{e_i[k]}{|\mathcal{N}_i^-[k]|+|\mathcal{N}_i^0[k]|}, & \text{if } j \in \mathcal{N}_i^-[k] \cup \mathcal{N}_i^0[k] \\ \frac{1}{2}\frac{e_i[k]}{|\mathcal{N}_i^+[k]|}, & \text{otherwise,} \end{cases}$$

if $|\Sigma_i^+[k]| > |\Sigma_i^-[k]|$.

[**Step** $s = 2$] During the previous step, it is possible that the antisymmetric requirement on F, i.e., $F = -F^{\mathrm{T}}$, may not be satisfied; thus, at Step 2, each node averages the value it computed for flow $f_{ij}[k+1,1]$ with the value computed by each adjacent node j, i.e., $f_{ji}[k+1,1]$. More specifically, each node i sends the value computed at the previous step to each $j \in \mathcal{N}_i$ and then updates each of its flows as

$$f_{ij}[k+1,2] = \frac{1}{2}(f_{ij}[k+1,1] - f_{ji}[k+1,1]).$$

[**Step** $s = 3$] For each incident flow, each node i compares its currently computed value for $f_{ij}[k+1,2]$ to the limits of the flow on that line as specified above. If the flow is outside the specified limits, it is clamped to its minimum or maximum, i.e., for each $j \in \mathcal{N}_i$,

$$f_{ij}[k+1,3] = \begin{cases} \underline{f}_{ij}, & \text{if } f_{ij}[k+1,2] < \underline{f}_{ij}, \\ \overline{f}_{ij}, & \text{if } f_{ij}[k+1,2] > \overline{f}_{ij}, \\ f_{ij}[k+1,2], & \text{otherwise.} \end{cases}$$

Once convergence has been reached for the three-step iterative process described above, the generator nodes can use the flows originating at the auxiliary nodes to determine the set-points that satisfy the feasibility problem in (4). More specifically, for each $i \in \mathcal{V}_g$, the feasible set-point is given as $u_i^* = f_{ii'}$ for $i' \in \mathcal{V}_g'$.

Like the ratio-consensus algorithm, the one described above converges asymptotically, i.e., to compute a set of feasible flows, the process must extend over an infinite number of iterations. By executing this algorithm for a finite number of iterations, k_0, properly chosen based upon the connectivity of the network and the initial conditions, however, the error between the value of the computed flows and their asymptotic values, ϵ, can be made as small as desired.

While we do not have a proof for the convergence of Algorithm 1, we believe it can be obtained using a combination of the techniques in [13] and [14]. Specifically, [13] discusses

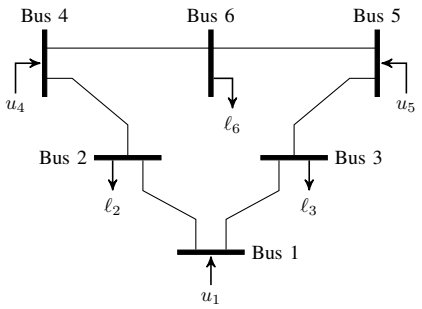

Fig. 1: One-line diagram of six-bus microgrid.

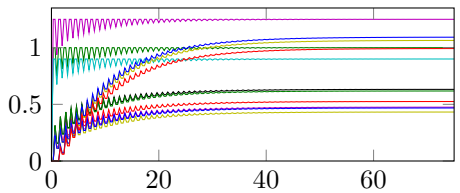

Fig. 2: Evolution of flows for $k = 0, 1, \ldots, 75$.

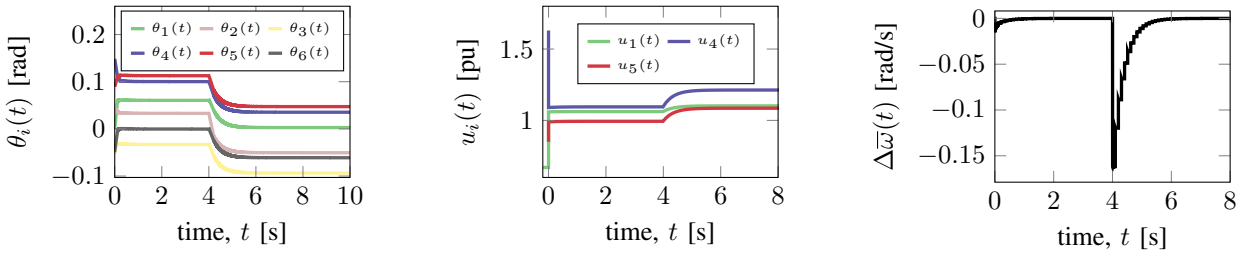

(a) Voltage angles. (b) Generator set-points. (c) Weighted average frequency error.

Fig. 3: Simulation results for six-bus microgrid pertrubed at $t = 4$ s.

how to obtain, in a distributed manner in a given directed graph, a set of weights that form a doubly stochastic matrix; each weight w_{ij} in the setting of [13] is constrained to be in the open interval $(0, 1)$ much like the flow f_{ij} on each edge in Algorithm 1 is constrained in the interval $[\underline{f}_{ij}, \overline{f}_{ij}]$ (and, of course, like Algorithm 1, a balance condition has to be satisfied at each node so that $\sum_{l\in\mathcal{N}_i^+} w_{li} = \sum_{j\in\mathcal{N}_i^-} w_{ij}$). Note that if one chooses any proper optimization criterion, then the techniques in [14], which are based on the results in [15], can be used to obtain an algorithm that solves the feasibility problem that Algorithm 1 attempts to solve (without paying attention to an optimization criterion).

V. Simulation Results

We demonstrate our proposed control scheme by simulating it on the six-bus ring microgrid shown in Fig. 1. As the diagram shows, the microgrid consists of 3 generators and 3 loads; initially, the generation set-points are $u = \begin{bmatrix} u_1, u_4, u_5 \end{bmatrix}^{\mathrm{T}} = \begin{bmatrix} 0.67, 1.63, 0.85 \end{bmatrix}^{\mathrm{T}}$, and the power demanded by each load is $\ell = \begin{bmatrix} \ell_2, \ell_3, \ell_6 \end{bmatrix}^{\mathrm{T}} = \begin{bmatrix} 1.0, 1.25, 0.9 \end{bmatrix}^{\mathrm{T}}$. We execute Algorithm 1 at the beginning of the simulation which yields new set-points, u^*. A plot of the flows as computed by the feasible flow algorithm is shown in Fig. 2 for $k_0 = 75$ iterations. After the algorithm is executed, the generators adjust their output such that they are operating at $u = u^* = \begin{bmatrix} 1.06, 1.1, 0.99 \end{bmatrix}^{\mathrm{T}}$. From Fig. 3, it can be seen that this adjustment results in a small transient in the system between approximately $t = 0$ and $t = 0.5$ s.

At $t = 4$ s, the amount of power demanded by the load at bus 6 is increased by 25% from 1.0 to 1.25. As shown in Fig. 3c, this results in a nonzero frequency error in the system which is eliminated by the control in (6) – (7). After approximately 2 seconds, i.e., at $t \approx 6$, the frequency is returned to the desired value and, as Fig. 3b shows, the generators have increased the amount of power they are outputting such that the total power demand is met.

VI. Concluding Remarks

In this paper, we presented a control architecture suitable for regulating the frequency in a microgrid such that the resulting operating point is stable and synchronized. Additionally, we proposed a distributed implementation of the control architecture that relies on local controllers present at each bus and a communication network connecting them. The distributed implementation we propose relies on two algorithms; the first serves to eliminate the weighted average frequency error in the system, while the second allows the generators to compute set-points that are known to result in stable and synchronized operation. Future work includes obtaining a convergence proof for Algorithm 1.

References

[1] A. Wood and B. Wollenberg, *Power Generation, Operation, and Control*. New York, NY: Wiley, 1996.

[2] M. Marwali, J.-W. Jung, and A. Keyhani, "Control of distributed generation systems - part II: Load sharing control," *IEEE Transactions on Power Electronics*, vol. 19, no. 6, pp. 1551–1561, Nov. 2004.

[3] J. W. Simpson-Porco, F. Dörfler, and F. Bullo, "Synchronization and power sharing for droop-controlled inverters in islanded microgrids," *Automatica*, vol. 49, no. 9, pp. 2603–2611, 2013.

[4] S. Cady, A. D. Domínguez-García, and C. N. Hadjicostis, "A distributed generation control architecture for islanded ac microgrids," *IEEE Transactions on Control Systems Technology*, 2015 (to appear).

[5] J. Peças Lopes, C. Moreira, and A. Madureira, "Defining control strategies for microgrids islanded operation," *IEEE Transactions on Power Systems*, vol. 21, no. 2, pp. 916–924, May 2006.

[6] M. Andreasson, D. Dimarogonas, K. Johansson, and H. Sandberg, "Distributed vs. centralized power systems frequency control," in *Proc. of European Control Conference*, 2013, pp. 3524–3529.

[7] A. Venkat, I. Hiskens, J. Rawlings, and S. Wright, "Distributed MPC strategies with application to power system automatic generation control," *IEEE Transactions on Control Systems Technology*, vol. 16, no. 6, pp. 1192–1206, 2008.

[8] F. Dörfler, J. W. Simpson-Porco, and F. Bullo, "Breaking the hierarchy: distributed control & economic optimality in microgrids," *IEEE Transactions on Control of Network Systems*, to appear.

[9] F. Dörfler, M. Chertkov, and F. Bullo, "Synchronization in complex oscillator networks and smart grids," *Proceedings of the National Academy of Sciences*, vol. 110, no. 6, pp. 2005–2010, 2013.

[10] A. D. Domínguez-García and C. N. Hadjicostis, "Distributed algorithms for control of demand response and distributed energy resources," in *Proc. of IEEE Conference on Decision and Control*, 2011, pp. 27–32.

[11] F. Dörfler and F. Bullo, "Synchronization in complex networks of phase oscillators: A survey," vol. 50, no. 6, pp. 1539–1564, 2014.

[12] S. T. Cady, A. D. Domínguez-García, and C. N. Hadjicostis, "Finite-time approximate consensus and its application to distributed frequency regulation in islanded ac microgrids," in *Proc. of Hawaii International Conference on System Sciences*, 2015, pp. 2664 – 2670.

[13] A. D. Domínguez-García and C. N. Hadjicostis, "Distributed matrix scaling and appplication to average consensus in directed graphs," *IEEE Transactions on Automatic Control*, vol. 58, no. 3, pp. 667–681, 2013.

[14] M. H. Schneider, "Matrix scaling, entropy minimisation, and conjugate duality (ii): The dual problem," *Mathematical Programming*, vol. 48, pp. 103–124, 1990.

[15] D. P. Bertsekas, P. A. Hosein, and P. Tseng, "Relaxation methods for network flow problems with convex arc costs," *SIAM Journal of Control and Optimization*, vol. 25, no. 5, pp. 1219–1243, 1987.